



Supplement of

The skill at modeling an extremely high ozone episode varies substantially amongst ensemble simulation

Jinhui Gao and Hui Xiao

Correspondence to: Hui Xiao (xh_8646@163.com)

The copyright of individual parts of the supplement might differ from the article licence.

Supplementary Information

Text S1: Model configuration and used data

Regarding the simulation settings (Fig. S1), we set up two nested domains with grids of 115×115 and 159×159 at horizontal resolution of 36 km and 12 km for the parent domain (D01) and nested domain (D02), respectively. D01 covers most parts of East and Southeast Asia where NIDA moved during its whole lifetime. D02 covers most parts of Middle and South China. There are 38 layers in vertical direction from surface to the upper pressure limit at 50 hPa. And 12 layers are set in the lowest 2km, whose simulation can describe more information of the atmosphere in PBL. The physics and chemistry parameterization settings of the simulation are listed in Table S1.

Multiple datasets are applied as input for the numerical simulation. The initial and boundary conditions of meteorology and chemistry are given by interpolating the National Centers for Environment Prediction (NCEP) final (FNL) operational global analysis data (<https://rda.ucar.edu/datasets/ds083.2/>) and the outputs of the Community Atmosphere Model with Chemistry (CAM-Chem; Lamarque et al., 2012; <https://www.acom.ucar.edu/cam-chem/cam-chem.shtml>). For the emissions, the anthropogenic emissions are provided by the Multi-resolution Emission Inventory for China (MEIC; Li et al., 2017; <http://meicmodel.org.cn/#firstPage>) that include five emission sectors (transportation, industry, power plant, residential combustion, and agricultural activity). The biogenic emissions are calculated by using the Model of Emissions of Gas and Aerosols from Nature (MEGAN; Guenther et al., 2006; <https://www.acom.ucar.edu/wrf-chem/download.shtml>). In addition, the observations of air pollutants (ozone and NO_2) and the meteorological factors are also collected for the model validation. The observation stations are distributed in the middle and south of China (Fig. S1b). The data at these stations is sufficient to evaluate the model performance on air pollutants and meteorology. The observations of air pollutants are measured and maintained by the China National Environmental Monitoring Center. The dataset can be downloaded from the website (<https://quotsoft.net/air/>). The observed meteorological factors at surface are temperature at 2m (T2), wind speed (WS) and wind direction (WD). They are measured by the China Meteorological Administration (CMA). We also collected the observations of wind sounds in GBA to evaluate the wind speed in vertical direction. Relevant information on the wind sound stations is listed in Table S2.

Table S1: Parameterization settings applied in this study.

| Item | Selection | Reference |
|--------------------------------|-------------------------------|------------------------|
| Microphysics | Lin | Lin et al. (1983) |
| Planetary Boundary Layer (PBL) | Yonsei University | Hong et al. (2006) |
| Land surface | Noah land surface | Chen and Dudhia (2001) |
| Surface layer | Monin-Obukhov | Zhang & Anthes (1982) |
| Urban physics | Single-layer UCM [§] | Kusaka et al. (2001) |
| Longwave radiation | RRTMG [*] | Iacono et al. (2000) |
| Shortwave radiation | RRTMG [*] | Iacono et al. (2000) |
| Gaseous chemistry | CBM-Z [#] | Zaveri & Peters (1999) |
| Dry deposition | Wesely | Wesely (1989) |
| Photolysis | Fast-J | Wild et al. (2000) |

^{*}RRTMG=Rapid Radiative Transfer Model for GCMs; [#]CBM-Z=Carbon Bond Mechanism Z; [§]UCM=Urban Canopy Model

Table S2: The codes and locations of the wind sound stations.

| CODE | LOCATION (Latitude, Longitude) |
|-------|--------------------------------|
| 59287 | 23.23° N, 113.50° E |
| 59476 | 22.53° N, 113.03° E |
| 59486 | 22.68° N, 114.21° E |
| G3239 | 22.70° N, 113.55° E |

30

Table S3: Model performances of good EMs and bad EMs on meteorological factors and NO₂ in and outside GBA.

| Variables | Region | IOA | | RMSE | | MNB | |
|-----------------|---------|----------|---------|----------|---------|----------|---------|
| | | Good EMs | Bad EMs | Good EMs | Bad EMs | Good EMs | Bad EMs |
| T2 | In GBA | 0.84 | 0.78 | 2.06 | 2.47 | -0.03 | 0.14 |
| | Outside | 0.83 | 0.83 | 2.52 | 2.51 | -0.43 | -0.35 |
| WS | In GBA | 0.49 | 0.36 | 1.62 | 2.36 | 75.07 | 117.78 |
| | Outside | 0.53 | 0.46 | 1.55 | 1.96 | 75.71 | 112.14 |
| WD | In GBA | 0.75 | 0.74 | 89.18 | 90.29 | 72.11 | 1.46 |
| | Outside | 0.79 | 0.76 | 81.20 | 87.20 | 26.75 | 24.43 |
| NO ₂ | In GBA | 0.66 | 0.64 | 20.76 | 19.76 | 7.26 | -5.49 |
| | Outside | 0.56 | 0.56 | 15.61 | 16.01 | 28.08 | 25.66 |

Table S4. The R, MNB and Index of each EM on ozone in the GBA

| EMs | R ($\times 100$) | MNB (%) | I_{dis} |
|------|--------------------|---------|-----------|
| EM01 | 86.23 | -30.97 | 33.90 |
| EM02 | 88.44 | -27.40 | 29.74 |
| EM03 | 90.67 | -32.58 | 33.89 |
| EM04 | 83.25 | -24.80 | 29.93 |
| EM05 | 90.79 | -21.42 | 23.32 |
| EM06 | 89.75 | -35.62 | 37.07 |
| EM07 | 86.60 | -34.00 | 36.77 |
| EM08 | 82.77 | -33.74 | 37.88 |
| EM09 | 88.52 | -31.62 | 33.64 |
| EM10 | 85.64 | -29.89 | 33.16 |
| EM11 | 88.48 | -32.46 | 34.44 |
| EM12 | 82.06 | -36.74 | 40.89 |
| EM13 | 92.30 | -23.47 | 24.70 |
| EM14 | 90.01 | -35.37 | 36.76 |
| EM15 | 85.06 | -28.46 | 32.14 |
| EM16 | 91.03 | -18.35 | 20.43 |
| EM17 | 92.08 | -10.92 | 13.49 |
| EM18 | 87.63 | -30.95 | 33.33 |
| EM19 | 83.59 | -31.34 | 35.37 |
| EM20 | 81.18 | -37.64 | 42.08 |
| EM21 | 84.54 | -30.11 | 33.85 |
| EM22 | 89.51 | -29.16 | 30.99 |
| EM23 | 85.15 | -46.99 | 49.28 |

| | | | |
|------|-------|--------|-------|
| EM24 | 86.04 | -26.11 | 29.60 |
| EM25 | 88.55 | -32.95 | 34.89 |
| EM26 | 87.68 | -29.10 | 31.60 |
| EM27 | 87.89 | -29.39 | 31.79 |
| EM28 | 81.99 | -40.32 | 44.16 |
| EM29 | 79.68 | -31.42 | 37.41 |
| EM30 | 89.28 | -28.72 | 30.66 |

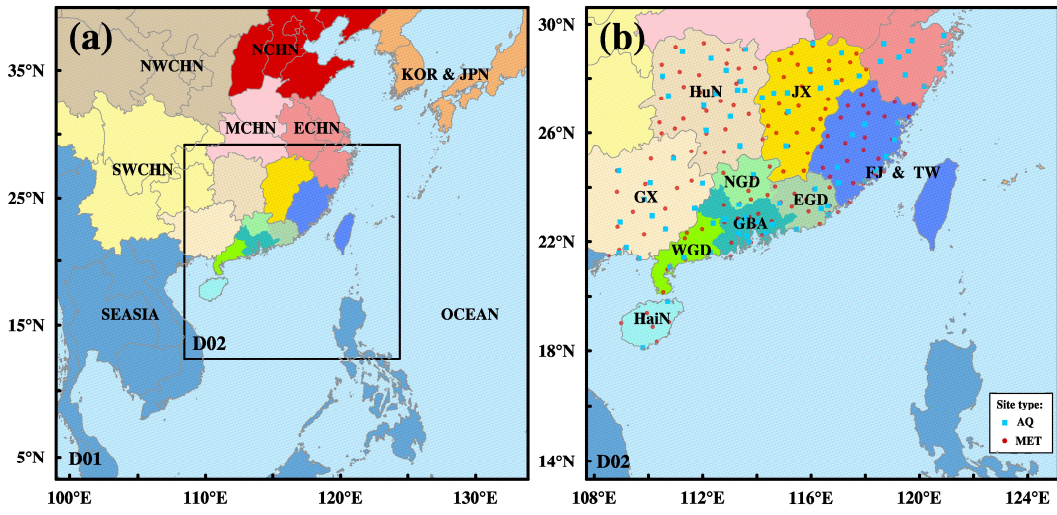
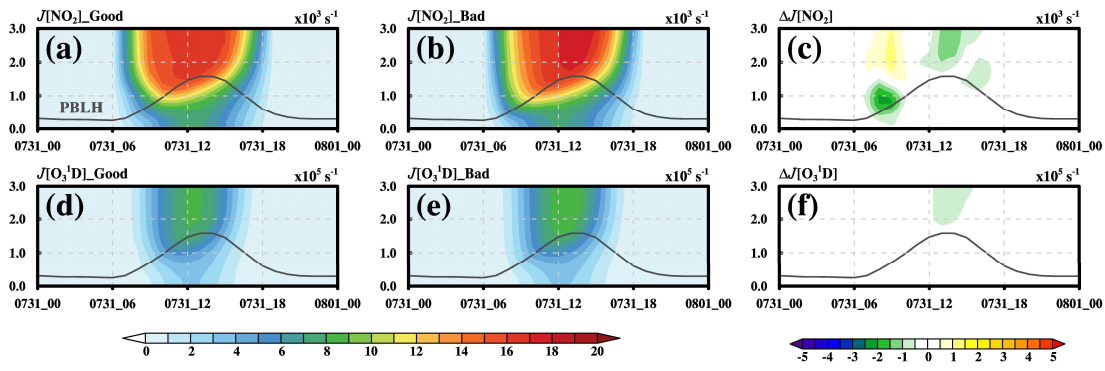


Figure S1: The model domain and the geographical source region setting.



40 Figure S2: the vertical distributions of photolysis rates and the differences between good and bad EMs.

References

- Chen, F. and Dudhia, J.: Coupling an advanced land surface hydrology model with the Penn State-NCAR MM5 modeling system. Part I: Model implementation and sensitivity, *Mon. Weather Rev.*, 129, 569–585, 2001.
- 45 Guenther, A., Karl, T., Harley, P., Wiedinmyer, C., Palmer, P. I., and Geron, C.: Estimates of global terrestrial isoprene emissions using MEGAN (Model of Emissions of Gases and Aerosols from Nature), *Atmos. Chem. Phys.*, 6, 3181–3210, <https://doi.org/10.5194/acp-6-3181-2006>, 2006.
- Hong, S. Y., Noh, Y., and Dudhia, J.: A new vertical diffusion package with an explicit treatment of entrainment processes, *Mon. Weather Rev.*, 134, 2318–2341, <https://doi.org/10.1175/Mwr3199.1>, 2006.
- 50 Iacono, M., Delamere, J., Mlawer, E., Shephard, M., Clough, S., and Collins, W.: Radiative forcing by long-lived greenhouse gases: Calculations with the AER radiative transfer models, *J. Geophys. Res.-Atmos.*, 113, D13103, <https://doi.org/10.1029/2008jd009944>, 2008.
- Kusaka, H., Kondo, H., Kikegawa, Y., Kimura, F.: A simple single-layer urban canopy model for atmospheric models: comparison with multi-layer and slab models. *Boundary-Layer Meteorol* 101:329 – 358, 2001.
- 55 Lamarque, J., Emmons, L., Hess, P., Kinnison, D., Tilmes, S., Vitt, F., Heald, C., Holland, E., Lauritzen, P., Neu, J., Orlando, J., Rasch, P., and Tyndall, G.: CAM-chem: description and evaluation of interactive atmospheric chemistry in the Community Earth System Model, *Geosci. Model Dev.*, 5, 369–411, <https://doi.org/10.5194/gmd-5-369-2012>, 2012.
- Li, M., Zhang, Q., Kurokawa, J., Woo, J., He, K., Lu, Z., Ohara, T., Song, Y., Streets, D., Carmichael, G., Cheng, Y., Hong, C., Huo, H., Jiang, X., Kang, S., Liu, F., Su, H., and Zheng, B.: MIX: a mosaic Asian anthropogenic emission inventory under the international collaboration framework of the MICS-Asia and HTAP, *Atmos. Chem. Phys.*, 17, 935–963, <https://doi.org/10.5194/acp-17-935-2017>, 2017.
- 60 Lin, Y., Farley, R., and Orville, H.: Bulk parameterization of the snow field in a cloud model, *J. Clim. Appl. Meteorol.*, 22, 1065–1092, [https://doi.org/10.1175/1520-0450\(1983\)022<1065:BPOTSF>2.0.CO;2](https://doi.org/10.1175/1520-0450(1983)022<1065:BPOTSF>2.0.CO;2), 1983.
- Wesely, M. L.: Parameterization of surface resistances to gaseous dry deposition in regional-scale numerical-models, *Atmos. Environ.*, 23, 1293–1304, [https://doi.org/10.1016/0004-6981\(89\)90153-4](https://doi.org/10.1016/0004-6981(89)90153-4), 1989.
- 65 Wild, O., Zhu, X., and Prather, M.: Fast-J: Accurate simulation of in- and below-cloud photolysis in tropospheric chemical models, *J. Atmos. Chem.*, 37, 245–282, <https://doi.org/10.1023/A:1006415919030>, 2000.
- Zaveri, R. and Peters, L.: A new lumped structure photochemical mechanism for large-scale applications, *J. Geophys. Res.-Atmos.*, 104, 30387–30415, <https://doi.org/10.1029/1999JD900876>, 1999.
- 70 Zhang, D., and Anthes, R.: A high-resolution model of the planetary boundary layer—Sensitivity tests and comparisons with SESAME-79 data. *Journal of Applied Meteorology*, 21(11), 1594–1609, [https://doi.org/10.1175/1520-0450\(1982\)021<1594:AHRMOT>2.0.CO;2](https://doi.org/10.1175/1520-0450(1982)021<1594:AHRMOT>2.0.CO;2), 1982.